AIAA JOURNAL
Vol. 41, No. 3, March 2003

Helmholtz-Like Resonator Self-Sustained Oscillations, Part 1: Acoustical Measurements and Analytical Models

S. Dequand,* X. Luo,† J. Willems,‡ and A. Hirschberg§
Eindhoven University of Technology, 5600 MB Eindhoven, The Netherlands

We consider self-sustained oscillations of the grazing flow along the neck of a Helmholtz-like resonator. Such oscillations are driven by a coupling between the intrinsic instability of the shear layer, separating the main flow from the cavity, and the resonant acoustical field in the cavity. Depending on details of the shape of the neck, acoustical velocities through the neck of the resonator of the same order of magnitude as the main flow velocity can be reached. For particular neck geometries, whistling is suppressed. A nonlinear model, which assumes that the vorticity of the shear layer is concentrated in line vortices traveling at constant velocity, provides insight into the phenomenon. For rounded edges, the model predicts the pulsation amplitude of the first hydrodynamic mode surprisingly well but severely overestimates the amplitude of higher hydrodynamic modes. For sharp edges, a modification of the original model is proposed, which yields a reasonable prediction of the pulsation amplitude (within a factor of two) of the first hydrodynamic mode and does not overestimate higher hydrodynamic modes.

Nomenclature

$C_{1,4}$	=	name of the studied configurations
c_0	=	speed of sound
$\mathrm{d}\xi/\mathrm{d}t$	=	mean acoustical velocity in neck of resonator
$\mathcal{F}$	=	aeroacoustical sources acting on the system
f	=	oscillation frequency
$\boldsymbol{f}_c$	=	Coriolis force density
f_0	=	resonance frequency
H	=	pipe width
h	=	parameter for calculation of sound absorption by vortex shedding at inner edge, 1 or 0.5
K	=	spring constant
L	=	cavity length
L_{eff}	=	effective length of the resonator
ℓ	=	distance between the settling chamber convergence and the upstream edge of the mouth of the resonator
M	=	mass
n	=	integer (index) representing the number of vortices shed at the upstream edge of the neck
$\mathcal{P}_{\mathrm{ac}}$	=	acoustical power generated by the sound source (vortex shedding at the upstream edge)
$\mathcal{P}_{\mathrm{down}}$	=	acoustical power due to vortex shedding at the downstream edge of the neck
$\mathcal{P}_{\mathrm{inner}}$	=	absorbed power due to vortex shedding at inner edges of the neck
P_0	=	wind-tunnel blowing pressure
p'	=	acoustical pressure at the top of the cavity
p'_{exp}	=	amplitude of the measured acoustical pressure at the top of the cavity, $\lvert p'(L)\rvert$
$p^\star$	=	ratio of the acoustical pressure p' at the top of the cavity and its measured amplitude p'_{exp}
$\langle p\rangle$	=	mean static pressure in the cavity
Q_f	=	measured quality factor of the system
R	=	damping coefficient related to the quality factor of the system
Re_ℓ	=	Reynolds number based on the distance ℓ
S	=	surface of integration
S_m	=	cross-sectional area of the mouth of the cavity
S_n	=	cross-sectional area of the neck
Sr	=	Strouhal number based on mouth width W
Sr_θ	=	Strouhal number based on momentum thickness θ of shear layer
T	=	oscillation period
T'	=	time needed by a vortex to travel through neck of the resonator
t	=	time
$\boldsymbol{U}$	=	steady potential flow velocity
U_Γ	=	velocity of the discrete vortices
U_0	=	main flow velocity amplitude
$\boldsymbol{u}_{\mathrm{rot}}$	=	rotational part of the velocity field
$\boldsymbol{u}'$	=	local acoustical velocity
u'_y	=	component in the y direction of local potential flow vector
V	=	absolute value of the local flow velocity
$\boldsymbol{V}$	=	local flow velocity
V_S	=	volume of integration
$V^\star$	=	ratio of velocity magnitude V and main flow velocity U_0
v	=	velocity in the complex plane
$\boldsymbol{v}$	=	velocity field
v_x	=	computed velocity component in x direction
v_y	=	computed velocity component in y direction
$v^\star$	=	complex conjugate of velocity v
$\lvert\boldsymbol{v}\rvert$	=	absolute value of the velocity field
W	=	neck width (mouth width)
x	=	coordinate in main flow direction
y	=	coordinate normal to flow
z	=	point coordinate in complex plane
α	=	opening angle of downstream edge of the neck
Γ	=	circulation of the point vortices representing vorticity field
Γ_d	=	circulation of point vortices shed at the downstream edge of neck
Γ_u	=	circulation of point vortices shed at upstream edge of the neck
Δp	=	discontinuity of pressure in the neck
$\Delta\omega_{3\mathrm{dB}}$	=	width of resonance peak (at 3 dB)
δ	=	Dirac function
θ	=	momentum thickness of shear layer
κ	=	geometrical factor
ν	=	kinematic viscosity

Presented as Paper 2001-2251 at the AIAA/CEAS 7th Aeroacoustics Conference, Maastricht, The Netherlands, 28–30 May 2001; received 1 July 2001; revision received 16 October 2002; accepted for publication 21 October 2002.

*Postdoctoral Research Assistant, Faculty of Applied Physics, Postbus 513.
†Ph.D. Student, Faculty of Applied Physics, Postbus 513.
‡Senior Engineer, Faculty of Applied Physics, Postbus 513.
§Professor, Faculty of Applied Physics, Postbus 513.

ξ = acoustical particle displacement
ρ_0 = density of air
ω = vorticity field
ω_0 = resonance pulsation
$\langle\ \rangle$ = time averaging over an oscillation period

Introduction

We consider a subsonic grazing flow along a deep cavity as shown in Fig. 1. This is a generic model for aircraft cavities or a car with an open sunroof. In such applications, self-sustained oscillations are a nuisance. In other cases, whistling of such a resonator can be useful, for example, in stall control.[1] The cavity has a neck between the opening (mouth) and the rest of the cavity. This implies that the cavity will have, as a Helmholtz resonator, strongly nonharmonic resonance frequencies. The cavity is, however, not shallow enough to neglect wave propagation in the cavity, and we, therefore, call this a Helmholtz-like cavity. Near the lowest resonance frequency f_0, the cavity acts as a monochromator, and the oscillations are almost purely harmonic. This justifies a simplified description of the acoustical response of the system, as used in our further analysis.

As the grazing flow velocity U_0 increases, self-sustained oscillations appear in critical ranges of Strouhal numbers $Sr = fW/U_0$ based on the mouth width W in the streamwise direction. Self-sustained oscillations of such systems have been extensively studied.[2]

The first models proposed were based on linear stability analysis assuming the response of the shear layer, separating the grazing flow from the stagnant fluid in the cavity, to be described by the linear inviscid theory for infinite parallel flows. Such models provide predictions of critical Strouhal numbers for maxima of pulsation amplitudes. They also predict a cutoff of the shear layer response above a critical Strouhal number $Sr_\theta = f\theta/U_0$ based on the momentum thickness θ of the shear layer.[3] For low-amplitude pulsations, increasing the thickness of the upstream boundary layer by means of a spoiler does indeed suppress the oscillations.[4,5]

More formal linearized models have been initiated by Möhring[6] who considered cavities built out of thin plates and assumed infinitesimally thin shear layers. It now appears accepted that the flow separation at a sharp upstream edge is well described within the framework of an inviscid flow theory by a Kutta condition (see Refs. 7–10). The character of the flow singularity at the downstream edge, however, remains obscure.[7,11] Although mathematically very elegant, such models can never predict flow-induced oscillation amplitudes because they are linear models.

Our aim is to consider the performance of some simplified nonlinear models that provide a prediction of the amplitudes of self-sustained oscillations. The first example of such a model was proposed by Howe.[12] He assumed that the cavity oscillation is driven by acoustically induced vortex shedding at the downstream edge of the mouth of the cavity. As an alternative, Nelson et al.[13,14] proposed to represent the shear layer by discrete line vortices. These discrete vortices accumulate the vorticity shed at the upstream edge, while they move at a constant speed $U_\Gamma \approx 0.4U_0$ along a straight line between the edges of the mouth of the cavity. The predicted amplitudes for square-edged cavities are, however, a factor of three or four too large. Bruggeman et al.[5] identified the unrealistic head-on collision of a point vortex with the flow singularity at the sharp downstream edge as the cause of this shortcoming. This was confirmed by Howe.[7] Hirschberg[15] obtained an analytical prediction for the particular case that the acoustical field can be assumed to be uniform across the mouth of the cavity. This is a model of a cavity with smoothly rounded mouth edges. Mongeau et al.[16] proposed also a simple analytical model based on the Nelson et al.[14] model. For the recorder flute, Fabre et al.[17] and Verge et al.[18] argued that Howe's model[12] predicts an absorption that is equivalent to that of the quasi-steady flow model of van Wijngaarden.[19]

Experimental studies by Bruggeman et al.[5] and Panton[20] have demonstrated a spectacular effect of the geometry of the mouth and the neck of the cavity on the resonance pulsation amplitudes. In the present paper, we present additional experimental data. We discuss this behavior in terms of the Nelson et al.[14] model for the shear layer. The vortex shedding at the downstream edge is described either by use of Howe's[12] model or by use of a quasi-steady flow model that is also used to predict turbulent losses at the inner edge of the neck. In a companion paper,[21] we discuss results of detailed flow measurements and of numerical simulations.

After a survey of the main experimental results, the theory is summarized, and the results of the models are compared with experimental results.

Experimental Study

Experimental Setup

The experimental setup is shown in Fig. 1. The resonator is placed in a semi-anechoic room, 60 mm downstream of the outlet (with square cross-sectional area of 60×60 mm) of a silent wind tunnel. The resonator volume consists of an aluminum pipe of square cross-sectional area of $H^2 = 60 \times 60$ mm^2 and 2-mm wall thickness. Hence, we have a 60-mm thick jet blowing along the opening of the resonator. Metal plates of 3-mm wall thickness are glued on the pipe walls to reduce wall vibrations. The pipe is terminated by a piston in which a piezoelectrical transducer (PCB 116A with Kistler Charge amplifier Type 5007) is placed. The piston position can be varied and is determined within 1 mm.

The neck of the resonator is shaped by two blocks of aluminum (of 25 mm height), which can be changed (Fig. 2). It has the same lateral dimension H as the pipe. The distance W between the upstream and the downstream edges in the mouth plane (Fig. 3) is determined within 0.1 mm. We consider either sharp edges or "rounded" edges. Instead of actually rounding off the edges, the neck edges are chamfered at an angle of 45 deg. Edges are kept as sharp as possible

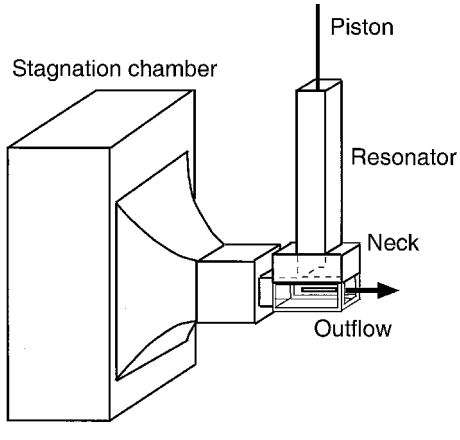

Fig. 1 Experimental setup.

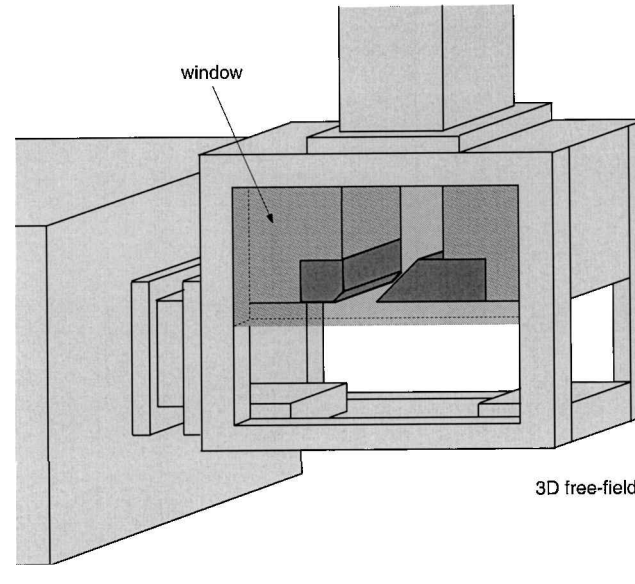

Fig. 2 Detail of experimental setup: neck of the resonator.

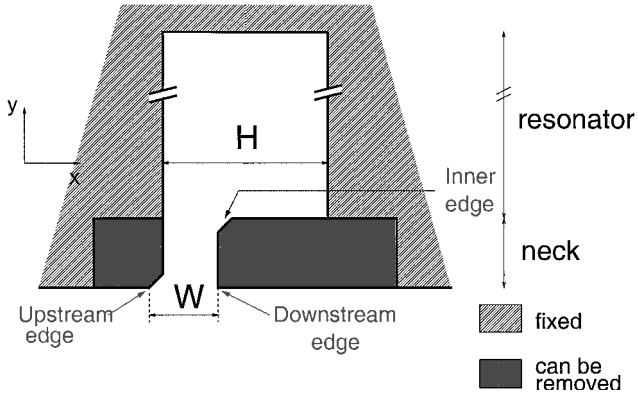

Fig. 3 Neck blocks.

(radius of curvature of the order of 10^{-5} m). We verified that such chamfered edges show aeroacoustical behavior very similar to that of rounded edges. The use of chamfered edges allows the simulation of flow separation by means of an inviscid flow computational method based on the Euler equations as discussed in the companion paper.[21]

Acoustical Measurements

During the acoustical measurements, the acoustical pressure $p'(t)$ at the top of the resonator, its frequency f, the length L of the resonator, and the main flow velocity U_0 were measured. The pressure signal $p'(t)$ measured at the top of the resonator volume is almost purely harmonic. Its frequency f was measured by means of a Philips frequency meter (Type PM 6671). Its amplitude p'_{exp} was deduced from rms voltage measurement of the charge amplifier output signal by means of a digital voltmeter.

The wind-tunnel blowing pressure P_0 was measured within 1-Pa accuracy by means of a Betz micromanometer. The main flow velocity U_0 was deduced from the reservoir pressure by using Bernoulli's formula $U_0 = \sqrt{(2P_0/\rho_0)}$ with density $\rho_0 = 1.2$ kg/m^3.

Because low frequencies are considered, only plane waves propagate in the resonator volume. In such a case, the acoustical velocity in the neck of the resonator is calculated from the measured acoustical pressure p' by means of the formula

$$\frac{\mathrm{d}\xi}{\mathrm{d}t} = \frac{H}{W}\frac{|p'_{\text{exp}}|}{\rho_0 c_0}\sin\left(\frac{2\pi f L}{c_0}\right)\sin(2\pi f t) \qquad (1)$$

in which $(\mathrm{d}\xi/\mathrm{d}t)$ represents the "mean" acoustical velocity in the neck defined as the acoustical volume flux divided by the mouth cross-sectional area WH. Here ξ is the acoustical particle displacement defined as positive when it is directed into the cavity. The global behavior of the dimensionless amplitude $|\mathrm{d}\xi/\mathrm{d}t|/U_0$ as a function of the Strouhal number $Sr = fW/U_0$ is, for a given neck geometry, independent of the resonator length L. Variations in $|\mathrm{d}\xi/\mathrm{d}t|/U_0$ as a function of L are smaller than 20%. Most of our measurements were therefore carried out at $L = 191$ mm. This corresponds to frequencies of the order of $f = 280$ Hz at which measurements of U_0 are accurate.

Effect of Edge Geometry

We distinguish three types of edges in the neck of the resonator (Fig. 3): the inner edge, the upstream edge of the mouth, and the downstream edge of the mouth. All of these edges have a strong influence on the flow behavior in the neck of the resonator. Most of the time, their effect can be explained qualitatively, and theoretical models will be introduced in the next section.

This section presents experimental results obtained from acoustical measurements for different neck geometries.

Inner Edge

Vortex shedding at inner edges can only induce acoustical energy losses because there is no main flow from which energy can be extracted. Figure 4 shows the effect of the presence of sharp or rounded inner edges. When the inner edge is sharp (squares), turbulent losses are more important than when the inner edge is rounded

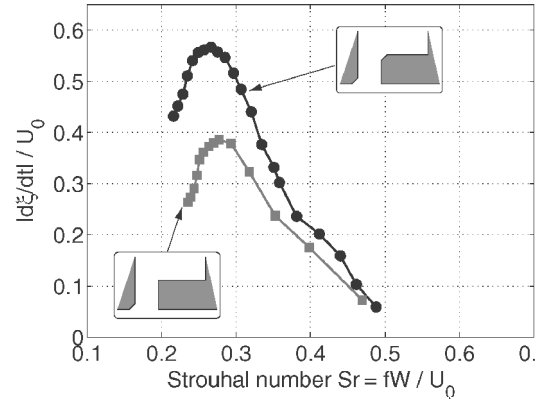

Fig. 4 Dimensionless acoustical velocity amplitude $|\mathrm{d}\xi/\mathrm{d}t|/U_0$ in the neck of the resonator as a function of the Strouhal number $Sr = fW/U_0$: effect of the inner edge (L = 190 mm).

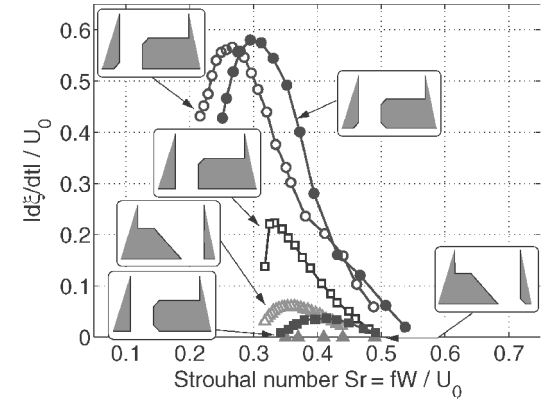

Fig. 5 Dimensionless acoustical velocity amplitude $|\mathrm{d}\xi/\mathrm{d}t|/U_0$ in the neck of the resonator as a function of the Strouhal number $Sr = fW/U_0$: effect of the upstream edge (L = 190 mm).

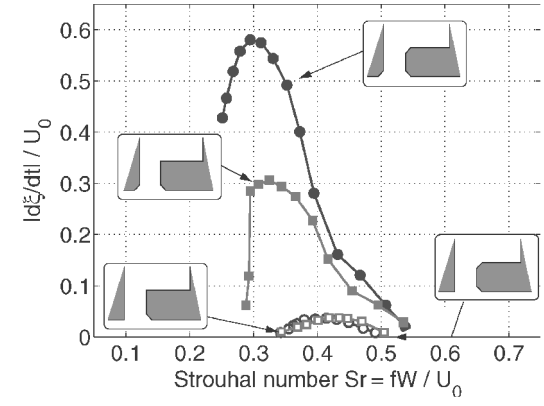

Fig. 6 Dimensionless acoustical velocity amplitude $|\mathrm{d}\xi/\mathrm{d}t|/U_0$ in the neck of the resonator as a function of the Strouhal number $Sr = fW/U_0$: effect of the upstream edge and of the inner edge (L = 190 mm).

or chamfered (circles). In the presence of a sharp inner edge, vortex shedding occurs both during in- and outflow of air through the neck. This explains qualitatively the differences in amplitude observed in Fig. 4.

Upstream Edge of the Mouth

When the upstream edge of the mouth is sharp, the initial acoustical absorption due to the vortex shedding can be very strong. This effect has been reported earlier by Bruggeman et al.[5] and Panton.[20] Figure 5 shows that this effect can even fully suppress the oscillations.

The effect of the upstream edge combines with the effect of the inner edge. Figure 6 shows the difference in amplitudes that occurs when, for a rounded downstream edge, we change the shape of the

other two edges. In this particular case, the presence of a sharp upstream edge reduces the pulsation amplitudes by more than a factor of four.

Downstream Edge of the Mouth

The effect of the geometry of the downstream edge is much more difficult to predict. Figure 7 shows experimental results for different opening angles α of the downstream edge. Again, the presence of a sharp edge will induce vortex shedding. However, it is not clear whether this vortex will absorb or produce acoustical energy. In his original study, Howe[12] proposed a model that predicted sound production due to this vortex shedding. We will argue in the next section that this vortex always absorbs acoustical energy. The sound production by vortices shed at the upstream edge can also be affected by the shape of the downstream edge.

The acoustical power is related to the acoustical velocity. When a vortex shed at the upstream edge reaches the downstream edge, it will produce acoustical energy if the acoustical velocity is negative $[(\mathrm{d}\xi/\mathrm{d}t)(t) < 0]$. The power generated is expected to increase with the reduction of the edge angle α because of the increased singularity of the local acoustical velocity field $\boldsymbol{u}'$ at the edge. That is what we observe for angles $45 \leq \alpha \leq 90$ deg in Fig. 7 with a kind of saturation at $\alpha = 45$ deg. For an opening angle $\alpha = 15$ deg, we observe a lower acoustical velocity amplitude. In this case, the acoustical energy absorbed by the vortex shed at the downstream edge is expected to be of the same order of magnitude as the acoustical energy produced by the vortex shed at the upstream edge. For the angle $\alpha = 90$ deg, a sudden decrease in amplitude is observed at low Strouhal numbers. This behavior is typical for low amplitude regime as explained by Bruggeman et al.[5]

When the upstream edge of the mouth is rounded, the effect of the opening angle of the downstream edge becomes much less significant (Fig. 8). This difference of behavior with that observed for a sharp upstream edge (Fig. 7) could indicate an absorption threshold below which the pulsation behavior is rather independent of the exact value of the absorption. Another explanation is that, in the case of a rounded upstream edge, the vortex path remains far remote from the downstream edge, whereas, for a sharp upstream edge, the vortex does interact with the downstream edge. Flow visualization shows this for Strouhal numbers around $Sr = 0.3$. We will see in Ref. 21 that this effect is predicted by an Euler flow simulation.

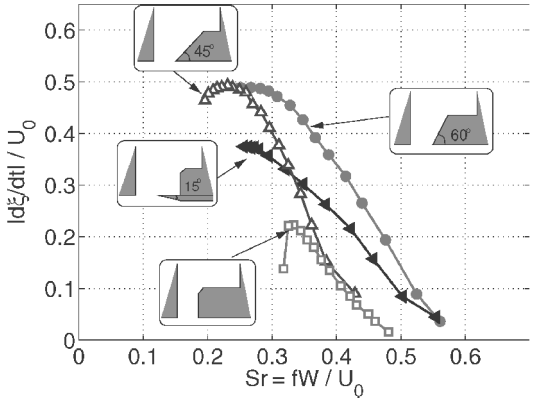

Fig. 7 Dimensionless acoustical velocity amplitude $|\mathrm{d}\xi/\mathrm{d}t|/U_0$ in the neck of the resonator as a function of the Strouhal number $Sr = fW/U_0$: effect of the downstream edge (L = 190 mm).

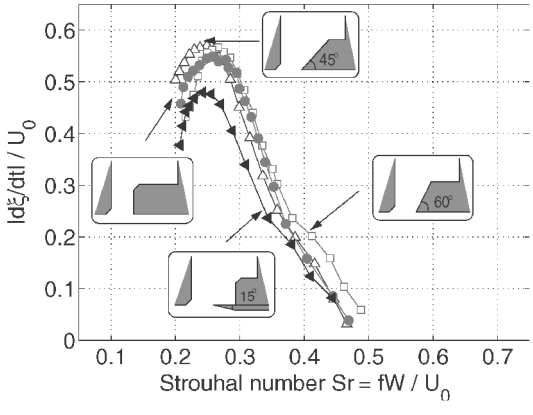

Fig. 8 Dimensionless acoustical velocity amplitude $|\mathrm{d}\xi/\mathrm{d}t|/U_0$ in the neck of the resonator as a function of the Strouhal number $Sr = fW/U_0$: effect of the downstream edge (L = 190 mm).

Theory

Vortex Sound

Our model is based on Howe's[7] generalization of Powell's[22] vortex-sound analogy. Howe's[7] key idea is that the local acoustical flow velocity $\boldsymbol{u}'$ is defined as the unsteady part of the potential flow component of the velocity field $\boldsymbol{v}$. In the low Mach number limit that we consider here, the source of sound appears to be the Coriolis force density

$$\boldsymbol{f}_c = -\rho_0(\boldsymbol{\omega} \times \boldsymbol{v}) \tag{2}$$

which an observer moving with a fluid particle experiences as a result of the vorticity $\boldsymbol{\omega} = \boldsymbol{\nabla} \times \boldsymbol{v}$. In this expression, the fluctuations in fluid density are neglected so that the density within the source region is taken as a constant ρ_0. When this level of approximation is used, the acoustical power $\mathcal{P}_{\mathrm{ac}}$ generated by this source is simply given by[23]

$$\mathcal{P}_{\mathrm{ac}} = \int_{V_s} \boldsymbol{f}_c \cdot \boldsymbol{u}' \, \mathrm{d}V \tag{3}$$

where the integration is taken over the source region of volume V_s.

A key point in the use of Howe's energy corollary[7] is that we simply ignore, in our model, spurious sound sources due to the time dependence of the circulation $\Gamma(t)$ of the point vortices representing the vorticity field. This time dependence would in an exact model induce a spurious discontinuity $\Delta p = -\rho_0(\partial\Gamma/\partial t)$ of the pressure across the feeding line between the vortex and the (sharp) edge from which vorticity is shed.

Vorticity Field

Howe[12] Model: Effect of the Downstream Edge

The model for the vortex shedding at the downstream edge is inspired by Howe's[12] model. The vortex is assumed to be induced by the acoustic flow. The vorticity is concentrated into a line vortex of strength Γ_d. This vortex imposes a Kutta condition at the downstream edge. In other words, the vortex strength is tuned to compensate the singularity of the potential acoustic flow at the downstream edge. When the vortex is outside the cavity, the vortex path is calculated by adding the effect of images of the vortex in the walls, to the convective main flow velocity (U_0, 0, 0). When the vortex is shed cavity inward, we ignore the effect of the main flow and set $U_0 = 0$ in Howe's model. As the vorticity Γ_d is tuned to remove the singularity of the acoustical flow at the downstream edge, the vortex vanishes each time the acoustical velocity $\mathrm{d}\xi/\mathrm{d}t$ changes sign. This implies that a new vortex is formed each time the velocity $\mathrm{d}\xi/\mathrm{d}t$ changes sign. This model was applied by Howe to a slit placed in an infinite plane with a grazing flow U_0 both above and below the slit (Fig. 9). In that case, Howe's approximate analytical solution predicted sound production.

Howe's analytical solution is compared (Fig. 9) to the solution obtained when his model is solved numerically for two time dependencies of the acoustical velocity: a square wave and a purely harmonic oscillation.

The acoustical energy $\langle \mathcal{P}_{\mathrm{ac}} \rangle / (\rho_0 U_0^2 |\mathrm{d}\xi/\mathrm{d}t| WH)$ (where $\langle\ \rangle$ denotes a time averaging over half a period of oscillations, which is the life time of a vortex) is plotted as a function of the dimensionless acoustical velocity $|\mathrm{d}\xi/\mathrm{d}t|/U_0$ (Fig. 9). We observe that the analytical solution (open square) predicts a sound production, whereas the numerical solution (filled symbols) predicts a sound absorption both for a square wave time dependence (filled square) and a sine wave time dependence (filled circle).

In all further calculations, we use the results of the numerical calculation with a sine wave time dependence. As already explained,

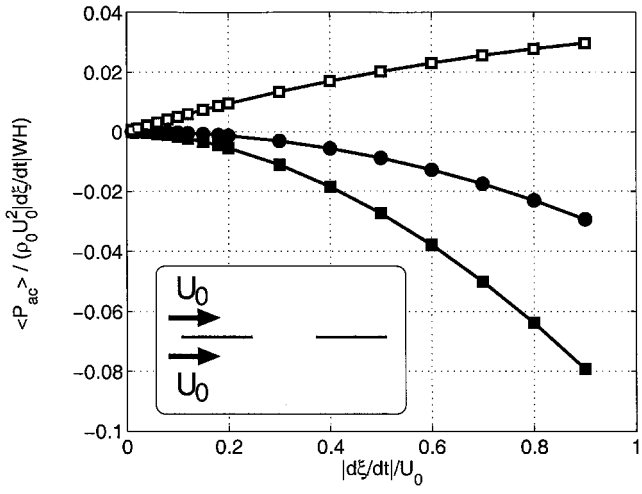

Fig. 9 Howe's[12] model for a slit geometry (calculations for a fixed Strouhal number $Sr = fW/U_0 = 0.25$); comparison between analytical and numerical solution: □, analytical square wave time dependence; ■, numerical square wave time dependence; and ●, numerical sine wave time dependence.

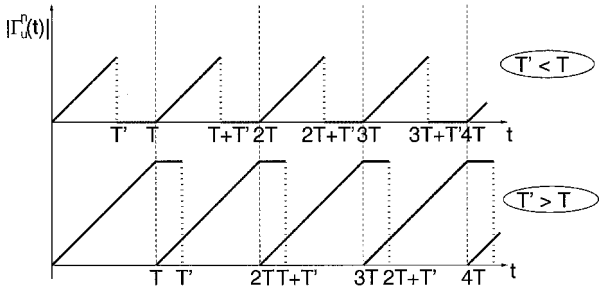

Fig. 10 Absolute value of the circulation $\Gamma_u^n(t)$ of individual vortices for two different main flow velocities, such as $T' < T$ and $T' > T$.

we assumed a grazing flow U_0 during half a period when $d\xi/dt < 0$, while we set $U_0 = 0$ in this model for $d\xi/dt > 0$. The slit case will only be used for comparison with experiments with a downstream-edge angle $\alpha = 15$ deg.

The model has also been applied to the square-edged geometry. The results are similar to those of the slit. Details of the results are presented by Dequand.[24]

Nelson et al.[14] Model: Effect of the Upstream Edge

The model proposed by Nelson et al.[14] assumes that the rate of vorticity shed at the upstream edge is given by

$$\frac{d\Gamma_u}{dt} = \frac{d\Gamma_u}{dx}\frac{dx}{dt} \approx \frac{U_0^2}{2} \tag{4}$$

In this formula, it is assumed that the vorticity is convected in the shear layer with an averaged velocity of $U_0/2$.

We assume that the vorticity of the shear layer is concentrated into point vortices of coordinates x_{Γ_u} and y_{Γ_u} traveling at a constant velocity $U_{\Gamma_u} = 0.4U_0$ on the straight line joining the upstream to the downstream edge. The acoustic field triggers the formation of a new vortex each oscillation period. Following Nelson et al. and Bruggeman et al.,[5] this formation corresponds to the moment at which the acoustical velocity $d\xi/dt$ changes sign from resonator outward to resonator inward. This is the moment $t_n = nT$, for $n = 0, 1, 2, \ldots$, at which the pressure at the top of the cavity reaches a minimum. Furthermore, it is assumed that, after a linear growth during the first period of its existence, the vortex reaches a final circulation that is kept constant (Fig. 10). The interaction between the vortex and the acoustic field is assumed to stop when the vortex reaches the downstream edge. We simply assume that the vortex is annihilated with its image in the wall as soon as it has passed the downstream edge. This model is described more in detail in earlier papers.[5,15] Figure 10 shows the absolute value of the circulation $\Gamma_u^n(t)$ of the nth vortex. $\Gamma_u^n(t)$ depends on the time $T' = H/U_{\Gamma_u}$ needed by the vortex to travel through the neck of the resonator.

Quasi-Steady Flow Models: Effect of the Inner Edge

In the presence of inner edges, turbulent losses due to the formation of secondary vortices appear. We describe this phenomenon by means of incompressible quasi-steady flow models as used earlier by Ingard and Ising[25] and van Wijngaarden.[19]

The neck of the resonator can be compared to a straight pipe. When the acoustic field enters the neck, the presence of an inner edge has the same effect as an open pipe and there is a jet formation driven by the acoustic flow, followed by a turbulent mixing region (Figs. 11a and 12a). When the acoustic velocity changes sign (each half oscillation period), the flow behavior depends on the geometry of the neck. If the inner edge is rounded, there is no flow separation (Fig. 12b). If the inner edge is sharp (Fig. 11b), a freejet that has a vena contracta is formed. We assume for simplicity a contraction factor of 0.5. Then, the jet flow becomes turbulent. This process is described by means of a quasi-steady flow model without wall friction.

By use of this model, the sound absorption by vortex shedding at the inner edge is given by

$$\langle \mathcal{P}_{\text{inner}} \rangle = \frac{1}{2}\rho_0 f_0 \int_0^{h/f_0} \iint_S \left|\frac{d\xi}{dt}\right| \left(\frac{d\xi}{dt}\right)^2 dS\, dt' \tag{5}$$

where f_0 is the resonance frequency.

When the inner edge is sharp (Fig. 11), turbulent losses are taken into account during one oscillation period ($h = 1$). When it is rounded (Fig. 12), turbulent losses are taken into account during half an oscillation period ($h = 0.5$). Equation (5) could also describe the sound absorption $\langle \mathcal{P}_{\text{down}} \rangle$ due to vortex shedding at the downstream

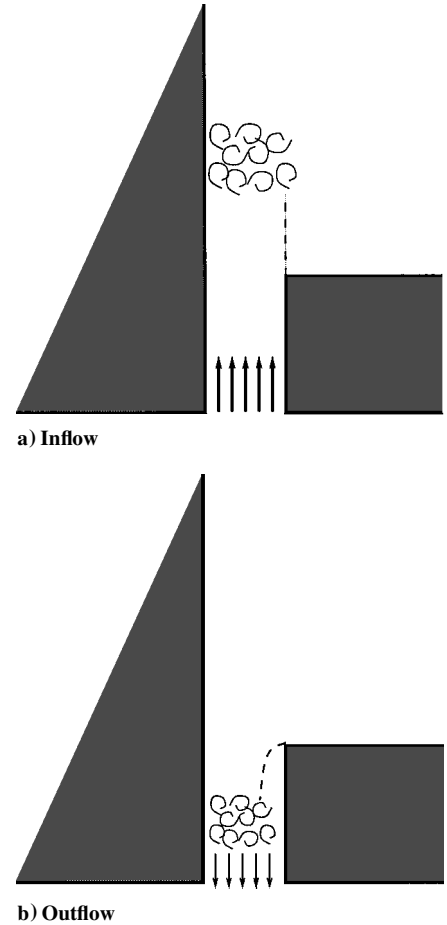

a) Inflow

b) Outflow

Fig. 11 Acoustically driven flow separation at the sharp inner edge of a neck.

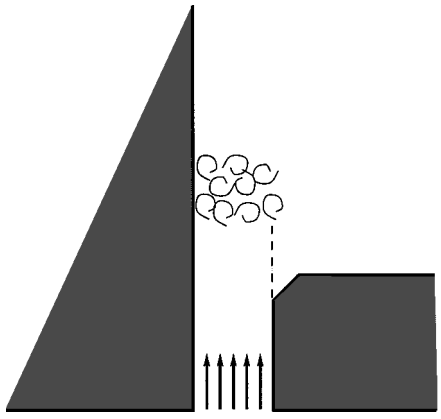

a) Inflow

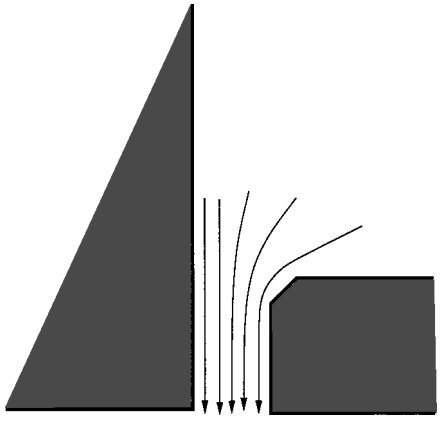

b) Outflow

Fig. 12 Acoustically driven flow separation at the rounded inner edge of a neck.

edge of the neck. We will compare this quasi-steady flow model to the point vortex model based on Howe's[12] model in the next section.

Simplified Model

Acoustical Model

The resonator can be described as a mass–spring system for which we have

$$M\frac{\mathrm{d}^2\xi}{\mathrm{d}t^2} + R\frac{\mathrm{d}\xi}{\mathrm{d}t} + K\xi = \mathcal{F}(t) \tag{6}$$

where $\mathcal{F}(t)$ corresponds to the aeroacoustical sources that act on the system and ξ is the mean acoustical displacement defined earlier. $\mathcal{F}(t)$ describes the effect of vortices and will be determined by means of the models presented in the preceding section.

The mass M and the damping coefficient R are determined from the passive acoustical response of the resonator in the absence of main flow. The damping coefficient R is related to the measured quality factor $Q_f = \omega_0/\Delta\omega_{3\mathrm{dB}} \approx 30$ of the system by

$$R = \omega_0 M/Q_f \tag{7}$$

The mass M is related to the effective length L_{eff} of the resonator. L_{eff} is determined by applying the mass conservation law between the neck and the resonator and is deduced from the measured resonance frequency f_0,

$$L_{\mathrm{eff}} = (W/H)(c_0/2\pi f_0)\cot[(2\pi f_0/c_0)L] \tag{8}$$

Then, the mass M of the system is calculated from

$$M = \rho_0 L_{\mathrm{eff}} HW \tag{9}$$

By definition, the resonance pulsation of the resonator is $\omega_0 = 2\pi f_0 = \sqrt{(K/M)}$. Therefore, the spring constant K is obtained from

$$K = (2\pi f_0)^2 \rho_0 L_{\mathrm{eff}} HW \tag{10}$$

We will further neglect departures of f from f_0.

Energy Balance

By multiplying Eq. (6) by $\mathrm{d}\xi/\mathrm{d}t$ and by averaging over one period of oscillation, we obtain the energy balance of the system

$$Rf_0\int_0^{1/f0}\left(\frac{\mathrm{d}\xi}{\mathrm{d}t}\right)^2\mathrm{d}t' + \langle\mathcal{P}_{\mathrm{inner}}\rangle + \langle\mathcal{P}_{\mathrm{down}}\rangle = f_0\int_0^{1/f_0}\iiint_{V_S}\boldsymbol{f}_c\cdot\left(\frac{\mathrm{d}\xi}{\mathrm{d}t}\right)\left[\boldsymbol{u}'\Big/\left(\frac{\mathrm{d}\xi}{\mathrm{d}t}\right)\right]\mathrm{d}\boldsymbol{y}\,\mathrm{d}t' \tag{11}$$

The left-hand side of Eq. (11) represents the acoustic energy absorbed as described in the preceding section and the right-hand side the acoustic energy produced by the system.

Because we assume that vortices are convected along a straight line and at a constant velocity $U_\Gamma = 0.4U_0$, the energy balance can be written as

$$Rf_0\int_0^{1/f_0}\left(\frac{\mathrm{d}\xi}{\mathrm{d}t}\right)^2\mathrm{d}t' + \langle\mathcal{P}_{\mathrm{inner}}\rangle + \langle\mathcal{P}_{\mathrm{down}}\rangle = U_{\Gamma_u}f_0\int_0^{1/f_0}\iiint_{V_S}\Gamma_u(t)\delta\big[x_{\Gamma_u}(t)\big]\delta\big[y_{\Gamma_u}(t)\big]\frac{u'_y}{\mathrm{d}\xi/\mathrm{d}t}\frac{\mathrm{d}\xi}{\mathrm{d}t}\,\mathrm{d}\boldsymbol{y}\,\mathrm{d}t'$$

$$= U_{\Gamma_u}Hf_0\int_0^{1/f_0}\Gamma_u(t)\frac{u'_y\big(x_{\Gamma_u},\,y_{\Gamma_u}\big)}{\mathrm{d}\xi/\mathrm{d}t}\frac{\mathrm{d}\xi}{\mathrm{d}t}\,\mathrm{d}t' \tag{12}$$

in which $\kappa = u'_y/(\mathrm{d}\xi/\mathrm{d}t)$ is a geometrical factor that relates the component in the y direction of the local potential flow vector u'_y to the acoustical flux $HW(\mathrm{d}\xi/\mathrm{d}t)$ through the neck.

Local Acoustical Field Geometrical Factor

When the neck edges are rounded, we assume that the geometrical factor $\kappa = u'_y/(\mathrm{d}\xi/\mathrm{d}t)$ is a constant[15]:

$$\kappa = S_n/S_m \tag{13}$$

where S_n is the cross-sectional area of the neck and $S_m = HW$ is the cross-sectional area of the mouth of the cavity along the vortex path (which takes into account the chamfers of the neck; Fig. 3).

When we want to take into account the effect of edges on the local acoustical flow distribution, we calculate κ by means of a conformal mapping. This is done by local potential flow calculations. Because we know that our model tends to overestimate the effect of the downstream singularity on the sound production by the vortex representing the shear layer, we will use the modified geometry shown in Fig. 13 to calculate the geometrical factor $\kappa = u'_y/(\mathrm{d}\xi/\mathrm{d}t)$. In this modified geometry, the downstream edge is replaced by a wall.

Near the singularity ($z = 0$), we know that the flow velocity behaves as $z^{-1/3}$ (Ref. 26). Therefore, we fit the solution to get an analytical expression of $\kappa(t)$. We find

$$\kappa(t) = aU_{\Gamma_u}^{-\frac{1}{3}}t^{-\frac{1}{3}} + b \tag{14}$$

where $a = 0.1941$ and $b = 0.2978$.

The proposed approach is quite arbitrary. Alternatives such as considering a different vortex path could also be considered.[7]

Results

Prediction of the Effect of Downstream Edge on Pulsation Amplitudes

Figures 14–16 compare the measured pulsation amplitudes to the prediction of the proposed analytical model. The continuous lines represent the data obtained when we use the numerical model based on Howe's[12] model to predict the effect of the downstream edge (see Theory section). The dashed lines represent the same calculation when the effect of the downstream edge is taken into account by using a quasi-steady flow model (as that used to predict the effect of the inner edge).

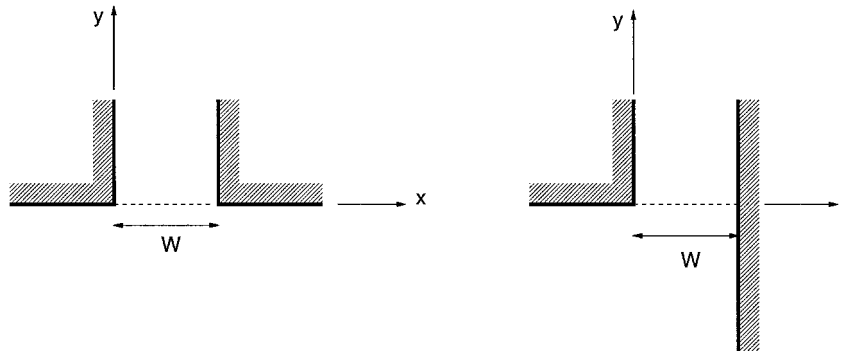

Actual Modified

Fig. 13 Geometry chosen to avoid the singularity of the downstream edge.

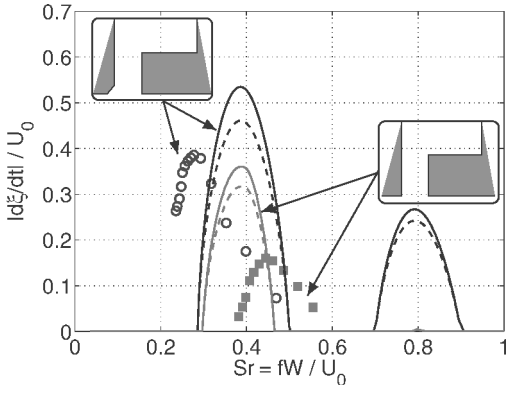

Fig. 14 Dimensionless acoustical velocity amplitude as a function of Strouhal number; comparison between experimental data and results of analytical models: ○, upstream edge rounded; ■, upstream edge sharp; ——, data obtained with Howe's[12] model to predict effect of downstream edge; and – – –, same calculation when effect of downstream edge is taken into account with a quasi-steady flow model.

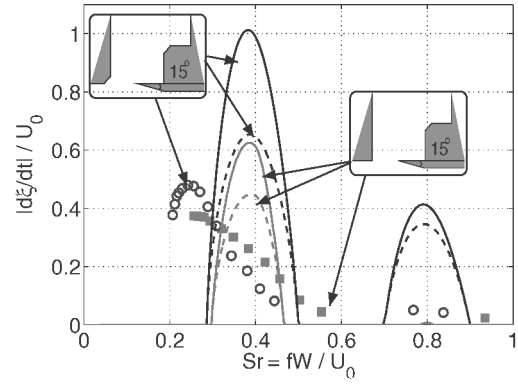

Fig. 16 Dimensionless acoustical velocity amplitude as a function of the Strouhal number; comparison between experimental data and results of analytical models: ○, upstream edge rounded; ■, upstream edge sharp; ——, data obtained with Howe's[12] model to predict effect of downstream edge; – – –, same calculation when effect of downstream edge is taken into account with a quasi-steady flow model.

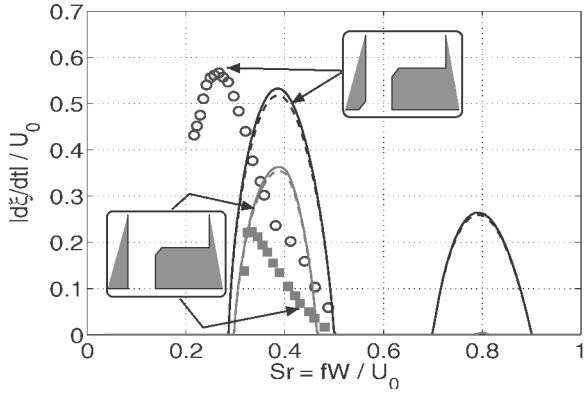

Fig. 15 Dimensionless acoustical velocity amplitude as a function of Strouhal number; comparison between experimental data and results of analytical models: ○, upstream edge rounded; ■, upstream edge sharp; ——, data obtained with Howe's[12] model to predict effect of downstream edge; and – – –, same calculation when effect of downstream edge is taken into account with a quasi-steady flow model.

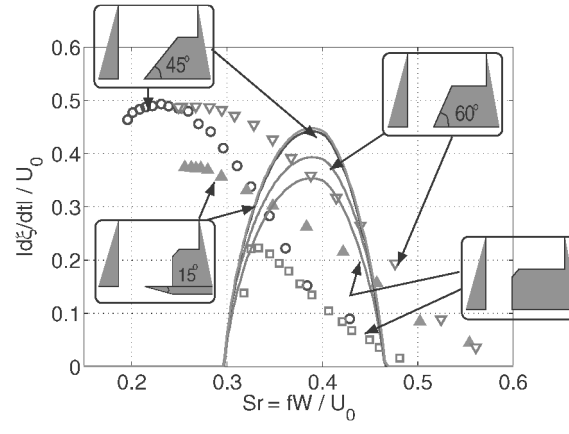

Fig. 17 Dimensionless acoustical velocity amplitude as a function of the Strouhal number; comparison between experimental data and results of analytical models: ——, data obtained when effect of downstream edge is taken into account by using a quasi-steady flow model.

For the $\alpha = 90$ deg geometry (Figs. 14 and 15), we observe that the pulsation amplitude is quite well predicted by the model when the upstream edge is rounded (circle). However, when the upstream edge is sharp (square), the model overestimates the amplitude by a factor of two. For these geometries, the predictions of Howe's[12] model and the quasi-steady flow model are equivalent.

Note that the model for rounded edges dramatically overestimates the amplitude of the second hydrodynamic mode at $Sr \approx 0.8$. The model for sharp edges does not show such unrealistic behavior at high Strouhal numbers.

When the downstream edge has an angle of 15 deg (Fig. 16), we use the Howe[12]-based model for the slit geometry. For this geometry, we observe that our model overestimates the pulsation amplitudes by a factor of 1.5–2. The quasi-steady flow model, with a vena contracta factor of 0.5, gives a better prediction. This result was unexpected. Indeed, we expected that the quasi-steady flow model would not be valid when the opening angle of the downstream edge decreases and that Howe's[12] model would provide a better description of the actual flow.

Limitations of the Model

The convective velocity of the vortices is actually amplitude dependent.[5] This explains that our model does not accurately predict the Strouhal number range in which pulsations occur. Furthermore, the model does not predict the effect of a variation in the shape of the downstream edge (Fig. 17).

Our quasi-steady flow model of the vortex shedding at the downstream edge does not take into account the different vena contracta effects that occur when the opening angle is different from 90 deg and could be improved.

Conclusions

Systematic acoustical measurements have been performed and have provided information about the influence of the neck geometry on self-sustained oscillations of a Helmholtz-like resonator. The effect of each edge can be described by means of analytical models. The effect of the upstream edge is rationalized by means of the Bruggeman et al.[5] and Hirschberg[15] implementations of the point vortex model of Nelson et al.[14] We propose a modification of these models to reduce the spurious effect of the collision of a point vortex with the downstream edge singularity. The presence of the inner edge is taken into account by means of quasi-steady flow models. The effect of the downstream edge can be described either by means of a numerical implementation of Howe's[12] model or by means of a quasi-steady flow model. The quasi-steady model gives results closer to experimental data, but the differences are not significant.

Comparisons between analytical and experimental data show that the pulsation amplitudes of the first hydrodynamic mode are reasonably predicted (within a factor of two). For rounded edges, the pulsation amplitudes of higher hydrodynamic modes are overestimated, whereas they almost vanish for sharp edges as observed in the experiments.

The proposed model is not able to describe quantitatively the flow behavior. In particular, the absence of effects of the downstream edge on the sound production for a rounded upstream edge cannot be understood with our simple models. This justifies the use of numerical simulations for a more detailed study of the flow. This is discussed in the companion paper.[21]

Acknowledgments

This work has been carried out within the framework of the European Project "Flow Duct Acoustics" (FLODAC, BRPR CT97-10394). The authors thank Robbie Balk and Lionel Hirschberg for carrying out a flow visualization study.

References

[1]Urzynicok, F., and Fernholz, H.-H., "Flow-Induced Acoustic Resonators for Separation Control," AIAA Paper 2002-2819, June 2002.

[2]Rockwell, D., and Naudasher, E., "Self-Sustained Oscillations of Flow Past Cavities," *Journal of Fluids Engineering*, Vol. 100, No. 2, 1978, pp. 152–165.

[3]Blake, W. K., *Mechanics of Flow-Induced Sound and Vibration, Volume 1: General Concepts and Elementary Sources*, Academic Press, Orlando, FL, 1986.

[4]Shaw, L. L., "Suppression of Aerodynamically Induced Cavity Pressure Oscillations," *Journal of the Acoustic Society of America*, Vol. 66, No. 3, 1979, pp. 880–884.

[5]Bruggeman, J. C., Hirschberg, A., van Dongen, M. E. H., Wijnands, A. P. J., and Gorter, J., "Flow Induced Pulsations in Gas Transport Systems: Analysis of the Influence of Closed Side Branches," *Journal of Fluids Engineering*, Vol. 111, No. 4, 1989, pp. 484–491.

[6]Möhring, W., "On Vortex Sound at Low Mach Number," *Journal of Fluid Mechanics*, Vol. 85, 1978, pp. 685–691.

[7]Howe, M. S., *Acoustics of Fluid–Structure Interactions*, Cambridge Univ. Press, Cambridge, England, U.K., 1998.

[8]Rienstra, S. W., "On the Acoustical Implications of Vortex Shedding from an Exhaust Pipe," *Journal of Engineering for Industry*, Vol. 103, No. 4, 1981, pp. 378–384.

[9]Bechert, D., "Excitation of Instability Waves in Free Shear Layers, Part 1: Theory," *Journal of Fluid Mechanics*, Vol. 186, 1988, pp. 47–62.

[10]Crighton, D. G., "The Kutta Condition in Unsteady Flow," *Annual Review of Fluid Mechanics*, Vol. 17, 1985, pp. 411–445.

[11]Crighton, D. G., "The Edge Tone Feedback Cycle, Linear Theory for the Operating Stages," *Journal of Fluid Mechanics*, Vol. 234, 1992, pp. 361–391.

[12]Howe, M. S., "Contributions to the Theory of Aerodynamic Sound, with Application to Excess Jet Noise and the Theory of the Flute," *Journal of Fluid Mechanics*, Vol. 71, No. 4, 1975, pp. 625–673.

[13]Nelson, P. A., Halliwell, N. A., and Doak, P. E., "Fluid Dynamics of a Flow Excited Resonance, Part 1: The Experiment," *Journal of Sound and Vibration*, Vol. 78, No. 1, 1981, pp. 15–38.

[14]Nelson, P. A., Halliwell, N. A., and Doak, P. E.,"Fluid Dynamics of a Flow Excited Resonance, Part 2: Flow Acoustic Interaction," *Journal of Sound and Vibration*, Vol. 91, No. 3, 1983, pp. 375–402.

[15]Hirschberg, A., "Aeroacoustics of Wind Instruments," *Mechanics of Musical Instruments*, edited by A. Hirschberg, J. Kergomard, and G. Weinrich, Springer-Verlag, Vienna, 1995, pp. 291–369.

[16]Mongeau, L., Kook, H., Brown, D. V., and Zorea, S. I., "Analysis of the Interior Pressure Oscillations Induced by Flow over Vehicle Openings," *Noise Control Engineering Journal*, Vol. 45, No. 6, 1997, pp. 223–234.

[17]Fabre, B., Hirschberg, A., and Wijnands, A. P. J., "Vortex Shedding in Steady Oscillations of a Flue Organ Pipe," *Acustica*, Vol. 82, No. 6, 1996, pp. 863–877.

[18]Verge, M. P., Fabre, B., Hirschberg, A., and Wijnands, A. P. J., "Sound Production in a Recorder-Like Instrument, Part 1: Dimensionless Amplitude of the Internal Acoustic Field," *Journal of the Acoustical Society of America*, Vol. 101, No. 5, 1997, pp. 2914–2924.

[19]Wijngaarden, L. van, "On the Oscillations near and at Resonance in Open Pipes," *Journal of Engineering Mathematics*, Vol. 2, No. 2, 1968, pp. 225–240.

[20]Panton, R. L., "Effect of Orifice Geometry on Helmholtz Resonator Excitation by Grazing Flow," *AIAA Journal*, Vol. 28, No. 1, 1989, pp. 60–65.

[21]Dequand, S., Hulshoff, S. J., van Kuijk, H., Willems, J., and Hirschberg, A., "Helmholtz-Like Resonator Self-Sustained Oscillations, Part 2: Detailed Flow Measurements and Numerical Simulations," *AIAA Journal*, Vol. 41, No. 3, 2003, pp. 416–423.

[22]Powell, A., "Theory of Vortex Sound," *Journal of the Acoustical Society of America*, Vol. 36, No. 1, 1964, pp. 177–195.

[23]Howe, M. S., "The Dissipation of Sound at an Edge," *Journal of Sound and Vibration*, Vol. 70, No. 3, 1980, pp. 407–411.

[24]Dequand, S., "Duct Aeroacoustics: From Technological Applications to the Flute," Ph.D., Dissertation, Faculty of Applied Physics, Eindhoven Univ. of Technology, Eindhoven, The Netherlands, and Univ. du Maine, Le Mans, France, Dec. 2001.

[25]Ingard, K. U., and Ising, H., "Acoustic Non-Linearity of an Orifice," *Journal of the Acoustical Society of America*, Vol. 42, No. 1, 1967, pp. 6–17.

[26]Prandtl, L., and Tietjens, O. G., *Fundamentals of Hydro- and Aeromechanics*, Dover, New York, 1934.

P. J. Morris
Associate Editor